HHS Public Access

Author manuscript

Biochemistry. Author manuscript; available in PMC 2022 October 15.

Published in final edited form as:

Biochemistry. 2021 December 21; 60(50): 3813–3821. doi:10.1021/acs.biochem.1c00615.

Insight into the phospholipid binding preferences of Kir3.4

Pei Qiao[1], **Samantha Schrecke**[2], **Jixing Lyu**[2], **Yun Zhu**[2], **Tianqi Zhang**[2], **Amanda Benavides**[2], **Arthur Laganowsky**[2,*]

[1]Department of Biochemistry and Biophysics, Texas A&M University, College Station, TX 77843

[2]Department of Chemistry, Texas A&M University, College Station, TX 77843

Abstract

The G-protein gated inwardly rectifying potassium channel 4 (Kir3.4) subunit forms functional tetramers. Previous studies have established that phosphatidylinositol 4,5-bisphosphate ($PI(4,5)P_2$) is required for Kir3.4 function. However, the binding preferences of Kir3.4 for the head group and acyl chains of phosphorylated phosphatidylinositides (PIPs) and other lipids is not well understood. Here, the interactions between full-length, human Kir3.4 and lipids are characterized using native mass spectrometry (MS) in conjunction with a soluble fluorescent lipid binding assay. Kir3.4 displays binding preferences for PIPs and, in some cases, the degree of binding is influenced by the type of acyl chains. The interactions between Kir3.4 and PIPs are weaker in comparison to full-length, human Kir3.2. The binding of $PI(4,5)P_2$ modified with a fluorophore to Kir3.2 can be enhanced by other lipids, such as phosphatidylcholine. Introduction of S143T, a mutation that enhances Kir3.4 activity, results in an overall reduction in the channel binding PIPs. In contrast, the D223N mutant of Kir3.4 that mimics the sodium bound state exhibited stronger binding for $PI(4,5)P_2$, particularly for those with 18:0–20:4 acyl chains. Taken together, these results provide additional insight into the interaction between Kir3.4 and lipids that are important for channel function.

Keywords

Potassium channel; phosphoinositides; lipid binding; native mass spectrometry; Förster resonance energy transfer

*Corresponding Author: ALaganowsky@chem.tamu.edu.

Author contributions

P.Q. and A.L. designed the research. P.Q. expressed and purified the protein. P.Q., S.S., J.L., Y.Z., T.Z., and A.B. prepared necessary chemicals and materials for experiments. P.Q. performed the experiments. P.Q. and A.L. analyzed the data. P.Q., S.S., J.L., Y.Z., T.Z., and A.L. wrote the manuscript.

Supporting Information

All experimental data are contained within the article or supporting information. Table S1–S2; Figures S1–S7.

Conflict of interest

The authors declare no competing financial interests.

Accession Codes

The accession ID for human Kir3.4 (KCNJ5) is P48544 and human Kir3.2 (KCNJ6) is P48051.

Introduction

Inward rectifying potassium (Kir) channels are found in cells throughout the human body, such as neuronal cells,[1] cardiac myocytes,[2] skeletal muscle cells,[3] blood cells,[4] and endothelial cells.[5] Kir channels have roles in numerous physiological functions, such as regulating the resting membrane potential of excitable cells,[6–8] parasympathetic slowing of the heart,[9] and pancreatic insulin secretion.[10] Dysfunction of Kir is associated with diseases, such as Bartter and Andersen syndromes.[11–14] The Kir channel family can be categorized into four groups based on their functional mechanism: K^+ transport channels (Kir1.x, Kir4.x, Kir5.x, and Kir7.x), constitutively active channels (Kir2.x), ATP-sensitive K^+ channels (Kir6.x), and G-protein-coupled Kir channels (Kir3.x).[3]

Despite their functional diversity, all of the Kir channels adopt a similar tetrameric structure with identical or different subunits.[15, 16] Each subunit consists of two cytoplasmic domains located on the N- and C-termini, and two transmembrane domains that are connected by a pore-forming P loop.[17] The function of Kir channels is regulated by many factors, such as ethanol, polyamines, magnesium, sodium, protein kinases, guanine nucleotide-binding proteins (G proteins), and phosphorylated phosphoinositides, such as $PI(4,5)P_2$.[18–25] The structures of Kir2.2 and Kir3.2 in complex with $PI(4,5)P_2$ have revealed $PI(4,5)P_2$ with 8:0 acyl chains binds to a specific site on each subunit.[26, 27] The binding site is located at the interface of the transmembrane domain and the cytoplasmic N-terminus, a highly conserved region that primarily consists of lysine and arginine residues. These positively charged amino acid residues interact with the phosphoglycerol backbone and the 4’ and 5’ phosphates of $PI(4,5)P_2$.[28, 29]

Besides $PI(4,5)P_2$, other PIPs can also activate Kir channels to different degrees.[30–32] In general, Kir2.x shows no stimulation by $PI(3,4)P_2$ and $PI(3,4,5)P_3$. Kir3.4 and Kir3.1/Kir3.4 have shown weak activation by $PI(3,4,5)P_3$ and $PI(3,4)P_2$. Kir6.2 is promiscuously activated by all PIPs.[19] In addition to the headgroups, different acyl chains of phosphoinositides also contribute to the regulation of Kir channel activity. The hetero-tetrameric Kir3.1/Kir3.4 channel shows specific selectivity for $PI(4,5)P_2$ with 18:0–20:4 acyl chains.[30, 33, 34] In contrast, Kir2.1 displays no preference for the lipid acyl chains.[35] Moreover, previous studies have shown that the activation of both Kir3.2 and Kir3.4 by $PI(4,5)P_2$ can be enhanced in the presence of sodium.[36–38] Anionic phospholipids, such as phosphatidic acid (PA), phosphatidylserine (PS), phosphatidylglycerol (PG), and phosphatidylinositol (PI) can also increase Kir2.1’s sensitivity to $PI(4,5)P_2$.[39, 40]

Native mass spectrometry (MS) is a powerful technique to interrogate membrane proteins and their interactions with ligands, such as lipids.[41–44] For example, native MS has identified lipids that stabilize membrane protein complexes.[45–48] It has also been used to determine the binding thermodynamics of protein-lipid interactions, as well as the allosteric coupling for protein-protein and protein-lipid interactions.[49–51] Native MS has also shown for a truncated form of Kir3.2 different affinities for PIPs with a preference for $PI(4,5)P_2$ headgroup.[52, 53] The headgroup binding preference determined by native MS is consistent with those obtained using a solution-based fluorescent lipid-binding assay in which binding

of a fluorophore-modified PI(4,5)P_2 to Kir3.2 fused to a fluorescent protein is monitored by Forster or Bioluminescent resonance energy transfer (FRET) measurements.[52, 54]

To better understand Kir-lipid interactions, we used native MS to characterize the binding of Kir3.4 and Kir3.2 to lipids varying in headgroup and acyl chain composition. Previous studies have determined lipid binding profiles for a truncated form of Kir3.2 from mouse.[55, 56] Here, lipid binding to full-length, human Kir3.4 and Kir3.2 is characterized. The results show Kir3.4 exhibits different lipid binding preferences. Interestingly, PIP binding of Kir3.4 is much weaker than that of Kir3.2. The S143T mutant that enhances Kir3.4 activity,[57] however, displayed an overall decrease in binding lipids. Kir3.4 containing the D223N mutation that mimics the sodium bound state[37] resulted in enhanced binding of PIPs with a preference for 18:0–20:4 acyl chains. These studies are also complemented with a competition soluble fluorescent lipid binding assay with results in line with those determined using native MS.

Materials and methods

Expression of full-length human Kir3.4 and Kir3.2.

Human Kir3.4 (KCNJ5, Uniprot P48544) and Kir3.2 (KCNJ6, Uniprot P48051) cDNA was obtained from Horizon with catalog numbers of MHS6278-202856496 and MHS6278-202857476, respectively. For native MS studies, the DNA corresponding to the full-length proteins was cloned into a modified pACEBac1 (Geneva Biotech) insect cell expression vector as a C-terminal fusion to a StrepTag II affinity tag. For fluorescent lipid binding assays, the full-length genes were cloned into a modified insect cell expression construct to express proteins with a tobacco etch virus (TEV) protease cleavable C-terminal fusion to mCherry and StrepTag II. The expression constructs were made by first amplifying genes by polymerase chain reaction using Q5 High-Fidelity DNA polymerase (New England Biolabs, NEB) and cloned into the modified insect cell expression vectors using HiFi DNA assembly kit (NEB) according to the manufacturer's protocol. The expression plasmids of this work have been deposited at Addgene plasmid #172425 to 172428. Mutants were introduced using the Q5 site-directed mutagenesis kit (NEB) according to the manufacturer's protocol. All expression plasmids were confirmed by DNA sequencing. The Kir3.2 and Kir3.4 expression constructs were transformed into *E. coli* DH10EMBacY (Geneva Biotech) following the manufacturer's protocol. Blue/White colony screening was used to identify clones that successfully incorporated the expression cassette into the baculoviral genome. A single, white colony was grown overnight and used for purification of bacmid DNA using a HiPure Plasmid Midiprep kit (Invitrogen). A single-step protocol was used for rapid baculovirus production.[58] In detail, the purified baculoviral DNA (30 μg) was incubated with PEI Max (Polysciences) transfection reagent (60 μl, 1 mg/ml) and 2ml PBS (NaCl 137 mM, KCl 2.7 mM, Na_2HPO_4 10 mM, KH_2PO_4 1.8 mM, pH 7.4) for 20 min. After 20 minutes of incubation at room temperature, the mixture was added directly to *Spodoptera frugiperda* (Sf9) cells (30 ml, 0.8×10^6 cell/ml) grown in suspension and incubated at 27 °C with shaking for seven days. The baculovirus was amplified in Sf9 following standard protocols. *Trichoplusia ni* (Tni) cells were used for protein expression

for 2–3 days post-infection. Insect cell lines and ESF 921 insect cell culture media were obtained from Expression Systems.

Protein purification and delipidation.

The Tni cells post-infection were harvested by centrifugation (4,000 g, 10 min). All purification steps were carried out at 4 °C unless otherwise stated. The cell pellets were resuspended in lysis buffer (50 mM TRIS, 300 mM potassium chloride, pH 7.4 at room temperature) and lysed by three passages through a microfluidizer (M-110PS, Microfluidics Inc.) operating at 25,000 psi. The cell lysate was clarified by centrifugation at 25,000 g for 20 min. Membranes were pelleted from the supernatant by ultra-centrifugation (100,000 g, 2 hours, 4 °C). The membrane pellets were resuspended in membrane resuspension buffer (30 mM TRIS, 150 mM potassium chloride, 10% Glycerol, pH 7.4 at room temperature) and homogenized using a glass homogenizer (Wheaton). Membrane proteins were extracted with 1.5% (w/v) n-Dodecyl-β-D-Maltopyranoside (DDM, Glycon Biochemicals) for two hours with gently stirring at 4 °C. The extracted membrane resuspension was clarified by centrifugation (40,000 g, 20min) and filtered through a 0.45 μm syringe filter. The protein sample was then loaded onto a drip column packed with 0.5 ml of Streptactin Sepharose (IBA Biosciences) pre-equilibrated with buffer SPKHA (50 mM Tris, 150 mM potassium chloride, 10% glycerol, and 0.025% DDM, pH 7.4 at room temperature). After loading, the column was washed with 5 column volumes (CV) of SPKHA, 10 CV of SPKHB buffer (50 mM Tris, 150 mM potassium chloride, 10% glycerol and 6 mM DHPC [1,2-dihepanoyl-sn-glycero-3-phosphocholine], pH7.4 at room temperature) to remove the co-purified contaminants, and 10 CVs of SPKHC buffer (50 mM Tris, 150 mM potassium chloride, 10% glycerol and 0.065% $C_{10}E_5$ [Pentaethylene Glycol Monodecyl Ether], pH 7.4). The protein was eluted with SPKHD buffer (SPKHC with 3 mM D-desthiobiotin). The concentration of protein was determined by using a DC protein assay (Bio-Rad).

Native mass spectrometry.

Protein samples were buffer exchanged into aqueous ammonium acetate (200 mM, pH 7.4 adjusted with ammonium hydroxide) supplemented with 0.065 % $C_{10}E_5$ using a centrifugal desalting column (Micro Bio-Spin 6, Bio-Rad). Lipid films were dissolved in the same buffer. Membrane protein samples were mixed with lipids at a molar ratio of 1:10 and analyzed on a Q Exactive UHMR Hybrid Quadrupole-Orbitrap mass spectrometer (Thermo). Gold-coated nanoelectrospray ionization emitters were prepared in-house as previously described.[59] Instrument settings were tuned to preserve non-covalent interactions as follows: the capillary voltage was 1.20 kV; the capillary temperature was 250 °C; collision-induced dissociation (CID) and collision energy (CE) was 60 V and 35 V, respectively; and detector mode and ion transfer target was set on high *m/z*. The in-source trapping mode was on with a desolvation voltage of −300 V. The trapping gas pressure was set at 7. Native MS was deconvoluted using UniDec[43] with the peak FWHM at 20.

Fluorescent lipid competition assay.

The fluorescent lipid BODIPY FL Phosphatidylinositol 4,5-bisphosphate (B-PIP, cat no. C-45F6) was purchased from Echelon Biosciences. The BODIPY fluorophore is affixed on the short acyl chain at the *sn*1 position. BODIPY is the donor that can excite the mCherry

fusion proteins through Förster resonance energy transfer (FRET) when the fluorescent lipid is bound to the protein. FRET measurements and correction factors were performed as previously described.[52] The experiments were conducted in SPKHC buffer. A total volume of 50 μl sample containing the protein and lipids was mixed at room temperature in a black 384-well plate (NUNC, cat no. 42761), and FRET measurements were made using a CLARIOstar microplate reader (BMG LABTECH).

Results

Preparation of full-length human Kir3.4 and Kir3.2 channels for native MS studies.

Human, full-length Kir3.4 and Kir3.2 with a C-terminal affinity tag were expressed and purified from insect cells for native MS characterization. The proteins were initially extracted and purified using n-Dodecyl-β-D-Maltopyranoside (DDM), a commonly used detergent. The native mass spectra of Kir channels displayed a broad hump and, in some cases, decorated with some sharp mass spectral peaks (Figure S1A, S2A). The underlying hump in the mass spectrum indicates the purified protein is heterogenous, which we speculate is the result of co-purified lipids. Nevertheless, the broad hump hinders the ability to resolve individual lipid binding events to the channel. In our previous studies[53, 56], we discovered that washing a truncated form of Kir3.2 immobilized on affinity resin with 1,2-dihepanoyl-sn-glycero-3-phosphocholine (DHPC), a short-chain lipid that forms micelles, removes co-purified contaminants resulting in pure samples. In a similar fashion, Kir3.4 and Kir3.2 were subjected to a DHPC wash to remove the contaminants. After this procedure, the native mass spectra of Kir channels in the pentaethylene glycol monodecyl ether ($C_{10}E_5$) detergent displayed a well-resolved mass spectrum with a measured mass in agreement with the theoretical mass of the tetrameric complex (Figure S1B, S2B; Table S2). Notably, the optimized samples provide means to resolve individual lipid binding events to the full-length channels.

Characterization of Kir3.4-lipid interactions.

The Kir3.4 samples devoid of co-purified contaminants were used to characterize lipid binding using native MS. The first set of lipids we investigated included phosphatidylinositol-3-phosphate (PI(3)P), PI(4)P, PI(5)P, PI(3,4)P_2, PI(4,5)P_2, and PI(3,4,5)P_3 with dioleoyl acyl chains (18:1–18:1, DO) and, for a subset, with 1-stearoyl-2-arachidonoyl (18:0–20:4, SA) acyl chains (Figure 1 and S3). Kir3.4 at a fixed concentration (0.5 μM) was mixed with 10 equivalents of lipid. For example, up to two lipid binding events were observed in the mass spectrum of the Kir3.4 in the presence of DOPI(4,5)P_2 (Figure 1B). Although the lipid bound mass spectral peaks are not base-line resolved, the small shifts in *m/z* for DOPI(4,5)P_2 (~1 kDa) binding to the intact Kir3.4 complex (~196 kDa) are readily discernable and these shifts are consistent with the mass of the lipid (Table S1, Figure S1). To compare the binding among lipids, the measured intensities from the deconvoluted mass spectra were used to determine the mole fraction of apo and lipid bound states (Figure 1C). For the mono phosphorylated PIPs, the total fraction of DOPI(3)P and DOPI(4)P bound Kir3.4 was similar, *i.e.*, similar abundance of apo, but the abundance of one and two lipids varied. Interestingly, PI(4)P with SA acyl chains resulted in a significant reduction in binding compared to this lipid with DO acyl chains. The total bound for

PI(3,4)P_2 and PI(4,5)P_2 lipids was similar and, like the PIPs with one phosphate, showed different abundances. For example, DOPI(4,5)P_2 had the highest abundance for one lipid bound whereas up to three SAPI(4,5)P_2 were bound to Kir3.4. PI(3,4,5)P_3 with SA acyl chains bound more to Kir3.4 in comparison to this lipid with DO acyl chains.

The second set of lipids characterized in this study focused on those with 1-palmitoyl-2-oleoyl (16:0–18:1, PO) acyl chains. This includes phosphatidylethanolamine (PE), phosphocholine (PC), phosphatidic acid (PA), phosphatidylserine (PS), phosphatidylglycerol (PG), and PI headgroups (Figure 1D, Table S1). Of the PO lipids, Kir3.4 bound up to two POPI molecules whereas only one binding event was observed for the other lipids. More POPE was bound to Kir3.4 followed by POPC and the least to POPA, POPS, and POPG. Interestingly, DOPI binds more avidly to Kir3.4 and at comparable levels to some PIPs. Moreover, the binding pattern of DOPI is suggestive of positive cooperativity.

Characterization of Kir3.2-lipid interaction.

To compare the Kir3.4-lipid interactions to other Kirs, we performed similar lipid binding studies for human Kir3.2 (Figure 2 and S4). In stark contrast to Kir3.4, native mass spectra reveal Kir3.2 binds avidly to PIPs and, in some cases, up to five lipid binding events were observed (Figure 2B). Kir3.2 robustly engages PI(4,5)P_2 with enhanced preference for the lipid with SA acyl chains (Figure 2C). Most interestingly, the binding pattern for DOPI(4,5)P_2, SAPI(4,5)P_2, and DOPI(3,4,5)P_3 suggests these lipids bind with positive cooperativity. The cooperative binding of DOPI(3,4,5)P_2 to Kir3.2 was diminished when the lipid contained SA acyl chain. Of the mono-phosphorylated PIPs, more PI(5)P was bound to the channel whereas binding for PI(3)P and PI(4)P are indistinguishable.

Next, the interactions of Kir3.2 with other phospholipids was characterized (Figure 2D). Unlike Kir3.4, the binding of POPI and DOPI was similar. Up to two POPE and POPS lipids were bound to Kir3.2. POPA while only one binding event was observed POPC and POPS. No binding between Kir3.2 and POPG was observed at the molar ratio tested.

Probing Kir-lipid interactions using fluorescent lipid competition assay.

A fluorescent lipid binding assay[52, 54] was employed to corroborate the findings from native MS measurements. To this end, samples of Kir3.4 and Kir3.2 with a monomeric red fluorescent protein (mCherry) fused to the C-terminus were prepared as done for native MS studies. Importantly, the optimized protein samples did not contain any co-purified contaminants (Figure S1, S2), which we have recently shown can impede specific lipid binding to truncated Kir3.2.[52] We then performed competition assays in which PI(4,5)P_2 containing a BODIPY fluorophore affixed to the acyl at the *sn*1 position (B-PIP) is competed off with natural lipids to compare with lipid binding profiles measured for the channels using native MS (Figure 3). The fluorescent lipid binding assay was performed with a fixed concentration of B-PIP and the addition of two equivalents of the phospholipid followed by recording the Förster resonance energy transfer (FRET) signal (Figure 3A, 3B). Of the PIPs tested, DOPI(3,4)P_2 and DOPI displayed a marginal reduction in FRET signal for Kir3.4. In general, the lipids weakly competed with the binding of B-PIP to Kir3.4, a result that agrees with the overall poor binding of lipids observed by native MS. For

Kir3.2, nearly half the FRET signal was lost in the presence of SAPI(4,5)P_2 followed by the same lipid with DO acyl chains. No competition was observed for Kir3.2 in the presence of DOPI, DOPI(4)P, DOPI(3,4)P_2 and SAPI(3,4,5)P_3, indicating relatively weak binding. Interestingly, some of the PO-type lipids, particularly PC, PA, PS and PG, enhanced the FRET signal indicating an enhancement in the interaction between Kir3.2 and B-PIP.

Characterization of mutant Kir3.4 channels with lipids.

We first prepared the Kir3.4 channel with the S143T mutation (Kir3.4^{S143T}) that has been shown to produce large inwardly rectifying, G-protein-modulated currents.[57] In a similar fashion as the wild-type channel, we performed native MS measurements of the mutant channel in the presence of different lipids (Figure 4 and S5). In general, the binding was largely weakened by this point mutation with a significant increase in abundance of the apo state (Figure 4C–D). SAPI(4,5)P_2 was the only lipid in which two lipid binding events to Kir3.4^{S143T} were observed. The binding profile of DOPI(3,4,5)P_3 was statistically indistinguishable from the wild-type protein (Figure 4C). A reduction of the binding of Kir3.4^{S143T} was observed for lipids with PO acyl chains (Figure 4D). More specifically, the binding of POPI and DOPI was considerably reduced compared to the avid binding of the wild-type protein.

The D223N mutant of Kir3.4 has been shown to mimic the sodium-bound state and strengthen the interaction with PI(4,5)P_2.[37] Native MS results for Kir3.4^{D223N} showed significant enhancement in PIPs binding (Figure 5 and S6). Interestingly, the PIPs with SA acyl chains bound more avidly compared to wild-type Kir3.4 (Figure 5C). For the DO type lipids, Kir3.4^{D223N} binding to DOPI(4,5)P_2 and DOPI(3,4,5)P_3 was similar to the wild-type protein. Compared to the wild-type channel, the binding of DOPI(4)P and DOPI(5)P was enhanced, and a reduction in binding DOPI(3)P and DOPI(3,4)P_2 was measured. A significant reduction was also observed for POPI and DOPI, lipids that bound avidly to Kir3.4. The binding of POPA and POPS was enhanced whereas a reduction in the binding of POPE, POPC, and POPG to Kir^{D223N}.

The FRET competition assay was also carried out for Kir3.4^{S143T} and Kir3.4^{D223N} (Figure S7). PI(4,5)P_2 with SA acyl chains competed the binding of B-PIP to Kir3.4^{D223N}. However, the binding of DOPI(4,5)P_2 to Kir3.4^{D223N} and PI(4,5)P2 binding to Kir3.4^{S143T} was statistically indistinguishable. These results are consistent with the native MS results where Kir3.4^{D223N} displays a higher affinity for PI(4,5)P_2 with SA tails.

Discussion

An important observation in this work is the rather weaker binding of Kir3.4 for PIPs in comparison to Kir3.2. The weak interaction between Kir3.4 and PIPs observed by native MS is in direct agreement with previous reports.[37, 57] Given Kirs are directly under PI(4,5)P_2 regulation, it is reasonable to speculate that the low activity is due to the channels' weak binding for PI(4,5)P_2. Interestingly, POPI and DOPI bind Kir3.4 with comparable or stronger binding than some PIPs. Kir3.2 binds PIPs more avidly and selectively compared to Kir3.4. The binding profiles for the Kir3.2 are reminiscent of our previous native MS studies using truncated mouse Kir3.2 conducted at a lower molar ratio of lipid to protein.[52, 53] The

most notable difference is Kir3.2 is more selective toward PIPs with a strong preference for the PI(4,5)P_2 head group and SA acyl chains. The enhanced selectivity toward PIPs along with acyl chain dependence suggests additional N- and C-terminal components of Kir3.2 influence specific lipid binding. Another interesting observation is the pronounced abundance of the fourth PI(4,5)P_2 bound to Kir3.2, indicating strong positive cooperativity in binding this lipid. The abundance of the fourth lipid bound state of Kir3.2 was also observed for DOPI(3,4,5)P_3.

Fluorescent lipid competition assays agree with native MS studies. Kir3.4 has shown an overall weaker binding profile for not only PIPs, but also almost all the lipids tested when compared to Kir3.2. For Kir3.2, DOPI(4,5)P_2 and SAPI(4,5)P_2 lipids show the strongest competition with B-PIP binding to Kir3.2. It is also interesting that POPA, POPC, POPS, and POPG enhances or allosterically modulates the interaction between B-PIP and Kir3.2 (p<0.05, students t-test). This observation is consistent with reports of anionic lipids significantly enhancing the sensitivity of Kir2.1 and Kir2.2 to PI(4,5)P_2.[31] However, a notable difference is the increase in B-PIP binding to Kir3.2 in the presence of POPC, a non-anionic lipid. Moreover, the enhancement in B-PIP binding to Kir3.2 in the presence of other lipids was not observed for the truncated, mouse Kir3.2.[52]

Kir3.4 can form functional homo-tetramers and its activity can be enhanced by the introduction of point mutations.[37, 57] The S143T mutation in Kir3.4 results in enhanced activity[60], however, we find the mutant channel does not possess increased binding for PIPs. In contrast, a pore helix mutation of Kir3.2 (E152D) was shown to increase channel activity and also enhance the interaction of PIP_2 with the mutant channel.[61, 62] The binding of $G_{\beta\gamma}$ to Kir1/4 hetero-tetramers has been shown to stabilize PIP_2 binding, suggesting the binding of these molecules to the channel is allosterically coupled.[18] Native MS studies were performed in the absence of $G_{\beta\gamma}$ and tight PIP binding may require the presence of $G_{\beta\gamma}$. It has been established that elevated levels of sodium (EC_{50} of 30–40 mM) activate Kir channels containing Kir3.2 or Kir3.4 subunits.[36–38, 63–65] Native MS studies cannot tolerate the high concentration of sodium needed to activate Kir3.2 or Kir3.4, which would result in significant adduction of sodium and mass spectral peak broadening. However, the D223N mutant of Kir3.4 mimics the effects of sodium on channel activity.[37] We find $Kir3.4^{D223N}$ shows increased PIP binding consistent with an earlier report.[37] A new finding is $Kir3.4^{D223N}$ displays enhanced the binding for PIPs with SA over DO acyl chains. In addition, the protein is more selective for PIPs as the binding to POPI and DOPI lipid was reduced compared to Kir3.4. Brain and heart PI(4,5)P_2 is predominantly found with SA tails and we find that Kir3.2 and Kir3.4 preferable binds SAPI(4,5)P_2 suggesting the channels have evolved to interact with this lipid.[66, 67] In summary, native MS and fluorescent lipid binding studies show that the selectivity of Kir3.2 and Kir3.4 (WT and mutants) toward PIPs depends not only on the headgroup but also the type of acyl chains.

Supplementary Material

Refer to Web version on PubMed Central for supplementary material.

Acknowledgments

We thank Dr. Thomas Meek, Dr. David Russell, and Dr. Pingwei Li for the useful discussion.

Funding and additional information

This work was supported by the National Institute of General Medical Sciences (NIGMS) of the National Institutes of Health (NIH) (DP2GM123486, R01GM121751, P41GM128577, and R01GM138863).

References:

[1]. Takahashi T (1990) Inward rectification in neonatal rat spinal motoneurones, J Physiol 423, 47–62. [PubMed: 2388157]

[2]. Kurachi Y (1985) Voltage-dependent activation of the inward-rectifier potassium channel in the ventricular cell membrane of guinea-pig heart, J Physiol 366, 365–385. [PubMed: 2414434]

[3]. Hibino H, Inanobe A, Furutani K, Murakami S, Findlay I, and Kurachi Y (2010) Inwardly rectifying potassium channels: their structure, function, and physiological roles, Physiol Rev 90, 291–366. [PubMed: 20086079]

[4]. Lewis DL, Ikeda SR, Aryee D, and Joho RH (1991) Expression of an inwardly rectifying K+ channel from rat basophilic leukemia cell mRNA in Xenopus oocytes, FEBS Lett 290, 17–21. [PubMed: 1915870]

[5]. Silver MR, and DeCoursey TE (1990) Intrinsic gating of inward rectifier in bovine pulmonary artery endothelial cells in the presence or absence of internal Mg2+, J Gen Physiol 96, 109–133. [PubMed: 2212977]

[6]. Chen R, and Swale DR (2018) Inwardly Rectifying Potassium (Kir) Channels Represent a Critical Ion Conductance Pathway in the Nervous Systems of Insects, Scientific Reports 8, 1617. [PubMed: 29371678]

[7]. Le Franc Y (2013) Inward Rectifier Potassium Channels, In Encyclopedia of Computational Neuroscience (Jaeger D, and Jung R, Eds.), pp 1–4, Springer New York, New York, NY.

[8]. Baronas VA, and Kurata HT (2014) Inward rectifiers and their regulation by endogenous polyamines, Frontiers in Physiology 5, 325. [PubMed: 25221519]

[9]. Touhara KK, Wang W, and MacKinnon R (2016) The GIRK1 subunit potentiates G protein activation of cardiac GIRK1/4 hetero-tetramers, Elife 5, e15750. [PubMed: 27074664]

[10]. Koster JC, Permutt MA, and Nichols CG (2005) Diabetes and insulin secretion: the ATP-sensitive K+ channel (K ATP) connection, Diabetes 54, 3065–3072. [PubMed: 16249427]

[11]. Simon DB, Karet FE, Rodriguez-Soriano J, Hamdan JH, DiPietro A, Trachtman H, Sanjad SA, and Lifton RP (1996) Genetic heterogeneity of Bartter's syndrome revealed by mutations in the K+ channel, ROMK, Nat Genet 14, 152–156. [PubMed: 8841184]

[12]. Jiao X, Ritter R III, Hejtmancik JF, and Edwards AO (2004) Genetic Linkage of Snowflake Vitreoretinal Degeneration to Chromosome 2q36, Investigative Ophthalmology & Visual Science 45, 4498–4503. [PubMed: 15557460]

[13]. Donaldson MR, Yoon G, Fu YH, and Ptacek LJ (2004) Andersen-Tawil syndrome: a model of clinical variability, pleiotropy, and genetic heterogeneity, Ann Med 36 Suppl 1, 92–97.

[14]. Reichold M, Zdebik AA, Lieberer E, Rapedius M, Schmidt K, Bandulik S, Sterner C, Tegtmeier I, Penton D, Baukrowitz T, Hulton SA, Witzgall R, Ben-Zeev B, Howie AJ, Kleta R, Bockenhauer D, and Warth R (2010) KCNJ10 gene mutations causing EAST syndrome (epilepsy, ataxia, sensorineural deafness, and tubulopathy) disrupt channel function, Proc Natl Acad Sci U S A 107, 14490–14495. [PubMed: 20651251]

[15]. Lyford LK, and Rosenberg RL (2003) Chapter 13 - Reconstitution in planar lipid bilayers of ion channels synthesized in ovo and in vitro, In Membrane Science and Technology (Tien HT, and Ottova-Leitmannova A, Eds.), pp 391–412, Elsevier.

[16]. Tristani-Firouzi M (2018) 94 - Andersen-Tawil Syndrome, In Cardiac Electrophysiology: From Cell to Bedside (Seventh Edition) (Zipes DP, Jalife J, and Stevenson WG, Eds.), pp 905–909, Elsevier.

[17]. Issa ZF, Miller JM, and Zipes DP (2019) 2 - Cardiac Ion Channels, In Clinical Arrhythmology and Electrophysiology (Third Edition) (Issa ZF, Miller JM, and Zipes DP, Eds.), pp 15–50, Elsevier, Philadelphia.

[18]. Huang CL, Feng S, and Hilgemann DW (1998) Direct activation of inward rectifier potassium channels by PIP2 and its stabilization by Gbetagamma, Nature 391, 803–806. [PubMed: 9486652]

[19]. Rohacs T, Lopes CM, Jin T, Ramdya PP, Molnar Z, and Logothetis DE (2003) Specificity of activation by phosphoinositides determines lipid regulation of Kir channels, Proc Natl Acad Sci U S A 100, 745–750. [PubMed: 12525701]

[20]. Fujiwara Y, and Kubo Y (2006) Regulation of the desensitization and ion selectivity of ATP-gated P2X2 channels by phosphoinositides, J Physiol 576, 135–149. [PubMed: 16857707]

[21]. McLaughlin Stuart, Wang Jiyao, Gambhir Alok, and Murray D (2002) PIP2 and Proteins: Interactions, Organization, and Information Flow, Annual Review of Biophysics and Biomolecular Structure 31, 151–175.

[22]. McLaughlin S, and Murray D (2005) Plasma membrane phosphoinositide organization by protein electrostatics, Nature 438, 605–611. [PubMed: 16319880]

[23]. Aryal P, Dvir H, Choe S, and Slesinger PA (2009) A discrete alcohol pocket involved in GIRK channel activation, Nat Neurosci 12, 988–995. [PubMed: 19561601]

[24]. Ruppersberg JP (2000) Intracellular regulation of inward rectifier K+ channels, Pflügers Archiv 441, 1–11. [PubMed: 11205046]

[25]. Sala-Rabanal M, Colin GN, and Crina MN (2015) Inward rectifying potassium channels, In Handbook of Ion Channels, CRC Press.

[26]. Hansen SB, Tao X, and MacKinnon R (2011) Structural basis of PIP2 activation of the classical inward rectifier K+ channel Kir2.2, Nature 477, 495–498. [PubMed: 21874019]

[27]. Whorton MR, and MacKinnon R (2011) Crystal structure of the mammalian GIRK2 K+ channel and gating regulation by G proteins, PIP2, and sodium, Cell 147, 199–208. [PubMed: 21962516]

[28]. Lee SJ, Ren F, Zangerl-Plessl EM, Heyman S, Stary-Weinzinger A, Yuan P, and Nichols CG (2016) Structural basis of control of inward rectifier Kir2 channel gating by bulk anionic phospholipids, J Gen Physiol 148, 227–237. [PubMed: 27527100]

[29]. Whorton MR, and MacKinnon R (2013) X-ray structure of the mammalian GIRK2-betagamma G-protein complex, Nature 498, 190–197. [PubMed: 23739333]

[30]. Rohacs T, Chen J, Prestwich GD, and Logothetis DE (1999) Distinct specificities of inwardly rectifying K(+) channels for phosphoinositides, J Biol Chem 274, 36065–36072. [PubMed: 10593888]

[31]. Cheng WWL, D'Avanzo N, Doyle DA, and Nichols CG (2011) Dual-mode phospholipid regulation of human inward rectifying potassium channels, Biophys J 100, 620–628. [PubMed: 21281576]

[32]. D'Avanzo N, Cheng WW, Doyle DA, and Nichols CG (2010) Direct and specific activation of human inward rectifier K+ channels by membrane phosphatidylinositol 4,5-bisphosphate, J Biol Chem 285, 37129–37132. [PubMed: 20921230]

[33]. Wenk MR, Lucast L, Di Paolo G, Romanelli AJ, Suchy SF, Nussbaum RL, Cline GW, Shulman GI, McMurray W, and De Camilli P (2003) Phosphoinositide profiling in complex lipid mixtures using electrospray ionization mass spectrometry, Nat Biotechnol 21, 813–817. [PubMed: 12808461]

[34]. Milne SB, Ivanova PT, DeCamp D, Hsueh RC, and Brown HA (2005) A targeted mass spectrometric analysis of phosphatidylinositol phosphate species, J Lipid Res 46, 1796–1802. [PubMed: 15897608]

[35]. D'Avanzo N, Lee S-J, Cheng WWL, and Nichols CG (2013) Energetics and location of phosphoinositide binding in human Kir2.1 channels, The Journal of biological chemistry 288, 16726–16737. [PubMed: 23564459]

[36]. Ho IH, and Murrell-Lagnado RD (1999) Molecular determinants for sodium-dependent activation of G protein-gated K+ channels, J Biol Chem 274, 8639–8648. [PubMed: 10085101]

[37]. Zhang H, He C, Yan X, Mirshahi T, and Logothetis DE (1999) Activation of inwardly rectifying K+ channels by distinct PtdIns(4,5)P2 interactions, Nat Cell Biol 1, 183–188. [PubMed: 10559906]

[38]. Ho IH, and Murrell-Lagnado RD (1999) Molecular mechanism for sodium-dependent activation of G protein-gated K+ channels, J Physiol 520 Pt 3, 645–651. [PubMed: 10545132]

[39]. Furst O, Mondou B, and D'Avanzo N (2014) Phosphoinositide regulation of inward rectifier potassium (Kir) channels, Front Physiol 4, 404. [PubMed: 24409153]

[40]. Cheng WWL, D'Avanzo N, Doyle DA, and Nichols CG (2011) Dual-Mode Phospholipid Regulation of Human Inward Rectifying Potassium Channels, Biophysical Journal 100, 620–628. [PubMed: 21281576]

[41]. Heck AJR (2008) Native mass spectrometry: a bridge between interactomics and structural biology, Nature Methods 5, 927–933. [PubMed: 18974734]

[42]. Liko I, Allison TM, Hopper JT, and Robinson CV (2016) Mass spectrometry guided structural biology, Curr Opin Struct Biol 40, 136–144. [PubMed: 27721169]

[43]. Marty MT, Baldwin AJ, Marklund EG, Hochberg GKA, Benesch JLP, and Robinson CV (2015) Bayesian Deconvolution of Mass and Ion Mobility Spectra: From Binary Interactions to Polydisperse Ensembles, Analytical Chemistry 87, 4370–4376. [PubMed: 25799115]

[44]. Agasid MT, and Robinson CV (2021) Probing membrane protein-lipid interactions, Curr Opin Struct Biol 69, 78–85. [PubMed: 33930613]

[45]. Laganowsky A, Reading E, Allison TM, Ulmschneider MB, Degiacomi MT, Baldwin AJ, and Robinson CV (2014) Membrane proteins bind lipids selectively to modulate their structure and function, Nature 510, 172–175. [PubMed: 24899312]

[46]. Gupta K, Donlan JAC, Hopper JTS, Uzdavinys P, Landreh M, Struwe WB, Drew D, Baldwin AJ, Stansfeld PJ, and Robinson CV (2017) The role of interfacial lipids in stabilizing membrane protein oligomers, Nature 541, 421–424. [PubMed: 28077870]

[47]. Allison TM, Reading E, Liko I, Baldwin AJ, Laganowsky A, and Robinson CV (2015) Quantifying the stabilizing effects of protein–ligand interactions in the gas phase, Nature Communications 6, 8551.

[48]. Fantin SM, Parson KF, Niu S, Liu J, Polasky DA, Dixit SM, Ferguson-Miller SM, and Ruotolo BT (2019) Collision Induced Unfolding Classifies Ligands Bound to the Integral Membrane Translocator Protein, Anal Chem 91, 15469–15476. [PubMed: 31743004]

[49]. Cong X, Liu Y, Liu W, Liang X, Russell DH, and Laganowsky A (2016) Determining Membrane Protein–Lipid Binding Thermodynamics Using Native Mass Spectrometry, Journal of the American Chemical Society 138, 4346–4349. [PubMed: 27015007]

[50]. Cong X, Liu Y, Liu W, Liang X, and Laganowsky A (2017) Allosteric modulation of protein-protein interactions by individual lipid binding events, Nature Communications 8, 2203.

[51]. Patrick JW, Boone CD, Liu W, Conover GM, Liu Y, Cong X, and Laganowsky A (2018) Allostery revealed within lipid binding events to membrane proteins, Proc Natl Acad Sci U S A 115, 2976–2981. [PubMed: 29507234]

[52]. Qiao P, Liu Y, Zhang T, Benavides A, and Laganowsky A (2020) Insight into the selectivity of Kir3.2 toward phosphatidylinositides, Biochemistry 59, 2089–2099. [PubMed: 32372643]

[53]. Liu Y, LoCaste CE, Liu W, Poltash ML, Russell DH, and Laganowsky A (2019) Selective binding of a toxin and phosphatidylinositides to a mammalian potassium channel, Nature Communications 10, 1352.

[54]. Cabanos C, Wang M, Han X, and Hansen SB (2017) A Soluble Fluorescent Binding Assay Reveals PIP2 Antagonism of TREK-1 Channels, Cell Rep 20, 1287–1294. [PubMed: 28793254]

[55]. Liu Y, LoCaste CE, Liu W, Poltash ML, Russell DH, and Laganowsky A (2019) Selective binding of a toxin and phosphatidylinositides to a mammalian potassium channel, Nat Commun 10, 1352. [PubMed: 30902995]

[56]. Qiao P, Liu Y, Zhang T, Benavides A, and Laganowsky A (2020) Insight into the selectivity of Kir3.2 toward phosphatidylinositides, Biochemistry.

[57]. Vivaudou M, Chan KW, Sui JL, Jan LY, Reuveny E, and Logothetis DE (1997) Probing the G-protein regulation of GIRK1 and GIRK4, the two subunits of the KACh channel, using functional homomeric mutants, J Biol Chem 272, 31553–31560. [PubMed: 9395492]

[58]. Scholz J, and Suppmann S (2017) A new single-step protocol for rapid baculovirus-driven protein production in insect cells, BMC Biotechnol 17, 83. [PubMed: 29145860]

[59]. Laganowsky A, Reading E, Hopper JT, and Robinson CV (2013) Mass spectrometry of intact membrane protein complexes, Nat Protoc 8, 639–651. [PubMed: 23471109]

[60]. Chan KW, Sui J-L, Vivaudou M, and Logothetis DE (1996) Control of channel activity through a unique amino acid residue of a G protein-gated inwardly rectifying K+ channel subunit, Proceedings of the National Academy of Sciences 93, 14193–14198.

[61]. Yi BA, Lin Y-F, Jan YN, and Jan LY (2001) Yeast Screen for Constitutively Active Mutant G Protein–Activated Potassium Channels, Neuron 29, 657–667. [PubMed: 11301025]

[62]. Adney SK, Ha J, Meng X-Y, Kawano T, and Logothetis DE (2015) A Critical Gating Switch at a Modulatory Site in Neuronal Kir3 Channels, The Journal of Neuroscience 35, 14397–14405. [PubMed: 26490875]

[63]. Lesage F, Guillemare E, Fink M, Duprat F, Heurteaux C, Fosset M, Romey G, Barhanin J, and Lazdunski M (1995) Molecular properties of neuronal G-protein-activated inwardly rectifying K+ channels, J Biol Chem 270, 28660–28667. [PubMed: 7499385]

[64]. Sui JL, Chan KW, and Logothetis DE (1996) Na+ activation of the muscarinic K+ channel by a G-protein-independent mechanism, J Gen Physiol 108, 381–391. [PubMed: 8923264]

[65]. Sui JL, Petit-Jacques J, and Logothetis DE (1998) Activation of the atrial KACh channel by the betagamma subunits of G proteins or intracellular Na+ ions depends on the presence of phosphatidylinositol phosphates, Proc Natl Acad Sci U S A 95, 1307–1312. [PubMed: 9448327]

[66]. Barneda D, Cosulich S, Stephens L, and Hawkins P (2019) How is the acyl chain composition of phosphoinositides created and does it matter?, Biochem Soc Trans 47, 1291–1305. [PubMed: 31657437]

[67]. Marsh D (2013) Handbook of Lipid Bilayers, Second Edition, CRC Press.

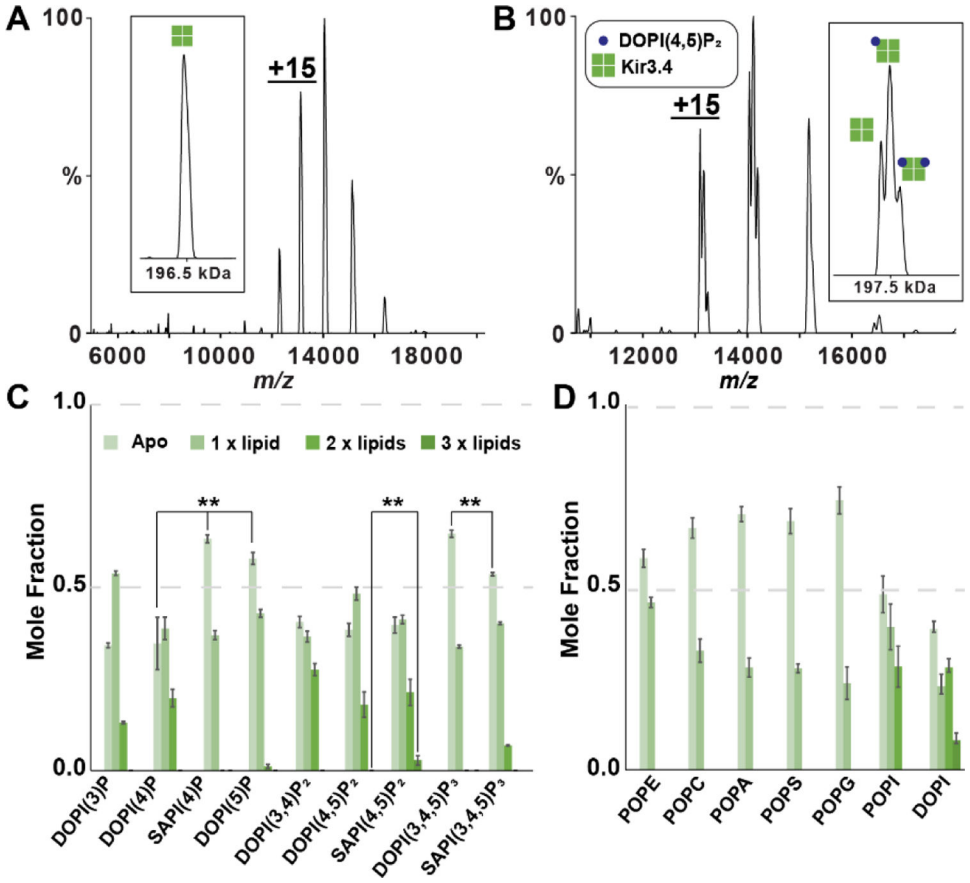

Figure 1. Biophysical characterization of Kir3.4-lipid interactions.

A) Representative native mass spectrum of optimized Kir3.4 samples solubilized in the $C_{10}E_5$ detergent. The deconvoluted mass spectrum is shown in the inset. B) Mass spectrum of 0.5 μM Kir3.4 mixed with 5 μM DOPI(4,5)P_2. Deconvolution of the mass spectrum is shown in the inset. C-D) Plot of mole fraction for individual binding events from deconvoluted native mass spectra of Kir3.4 in the presence of 10-fold molar excess of (C) PIPs and (D) phospholipids. Reported are the average and s.e.m. (n=3). For comparison, student's t test (** $p < 0.01$) was used with the mole fraction of the same lipid bound state. Lipid abbreviations are listed in Table S1.

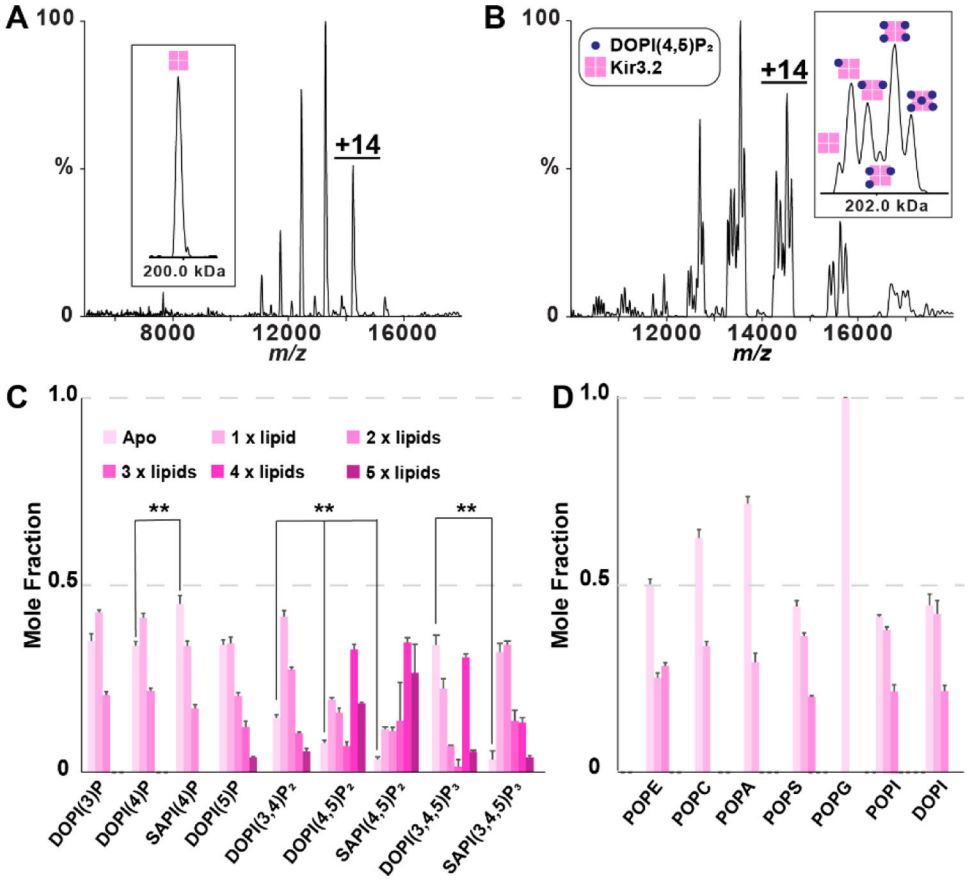

Figure 2. Native MS of human Kir3.2 in complex with phospholipids.

A) Representative native mass spectrum of Kir3.2 samples optimized for native MS. Shown as described in Figure 1. B) Mass spectrum of a mixture containing 0.5 μM Kir3.2 and 5 μM DOPI(4,5)P_2. The deconvoluted mass spectrum is shown in the inset. C-D) Plot of mole fraction for individual binding events from deconvoluted native mass spectra of Kir3.2 in the presence of 10-fold molar excess of (C) PIPs and (D) phospholipids. For comparison, student's *t* test (* *$p < 0.01$) was used with the apo mole fraction between indicated lipids. Reported are the average and s.e.m. (n=3).

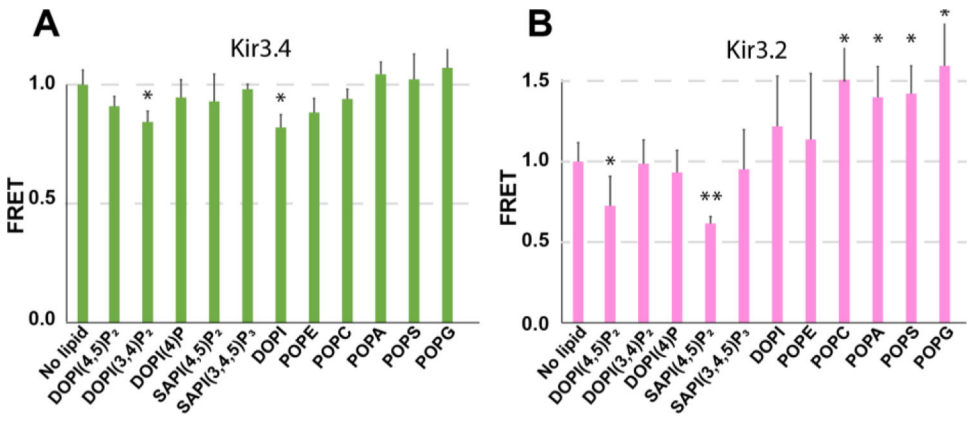

Figure 3. Kir3.4 and Kir3.2 fluorescent lipid binding and competition assays.

Competition of 0.5 μM (A) Kir3.4-mCherry and (B) Kir3.2-mCherry binding to B-PIP (4 μM) in the presence of 8 μM phospholipid. Lipid abbreviations are provided in Table S1. Reported are the average and s.e.m. (n=3). $^{*}p < 0.05$ and $^{**}p < 0.01$ compared to control (students t-test).

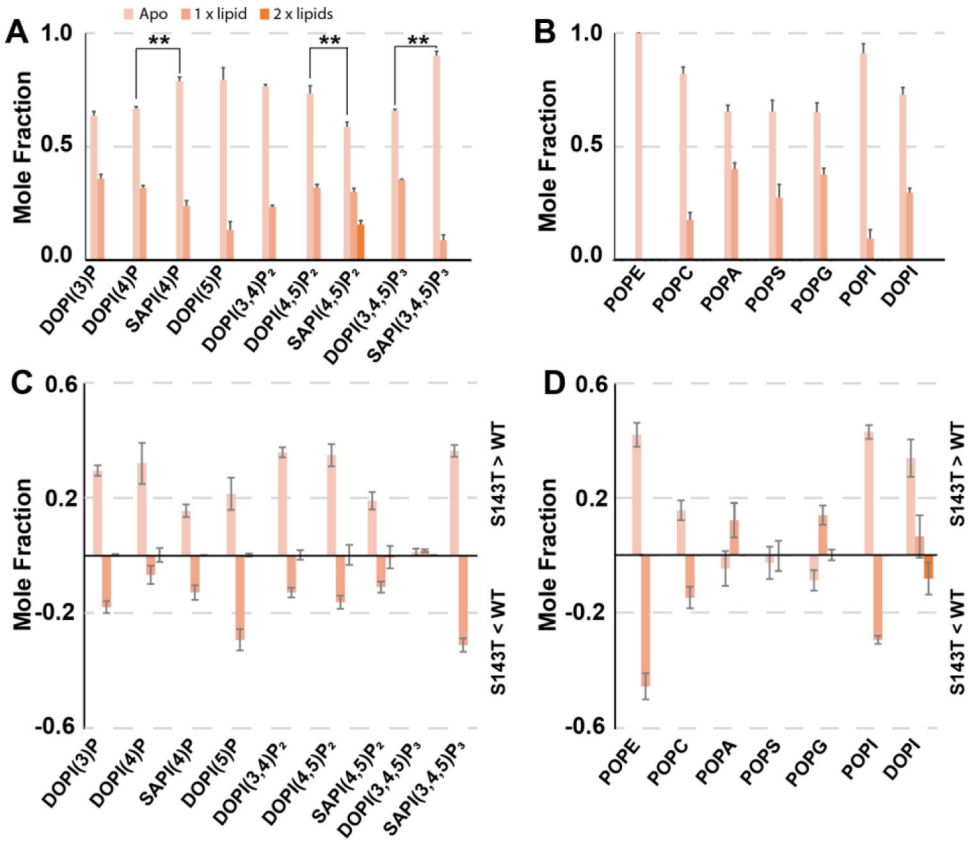

Figure 4. Kir3.4^{S143T} lipid interactions characterized by native MS.

A-B) Plot of mole fraction for of apo and lipid bound states of Kir3.4^{S143T} determined from the deconvoluted native mass spectra. Kir3.4^{S143T} was mixed with a 10-fold molar excess of (A) PIPs and (B) lipids. C-D) Plot of the difference in mole fraction of (C) PIPs and (D) lipids bound to Kir3.4^{S143T} from Kir3.4. Positive values indicate a higher mole fraction of the particular state for Kir3.4^{S143T}. For comparison, student's t test (* $p < 0.01$) was used with the apo mole fraction between indicated lipids. Reported are the average and s.e.m. (n=3).

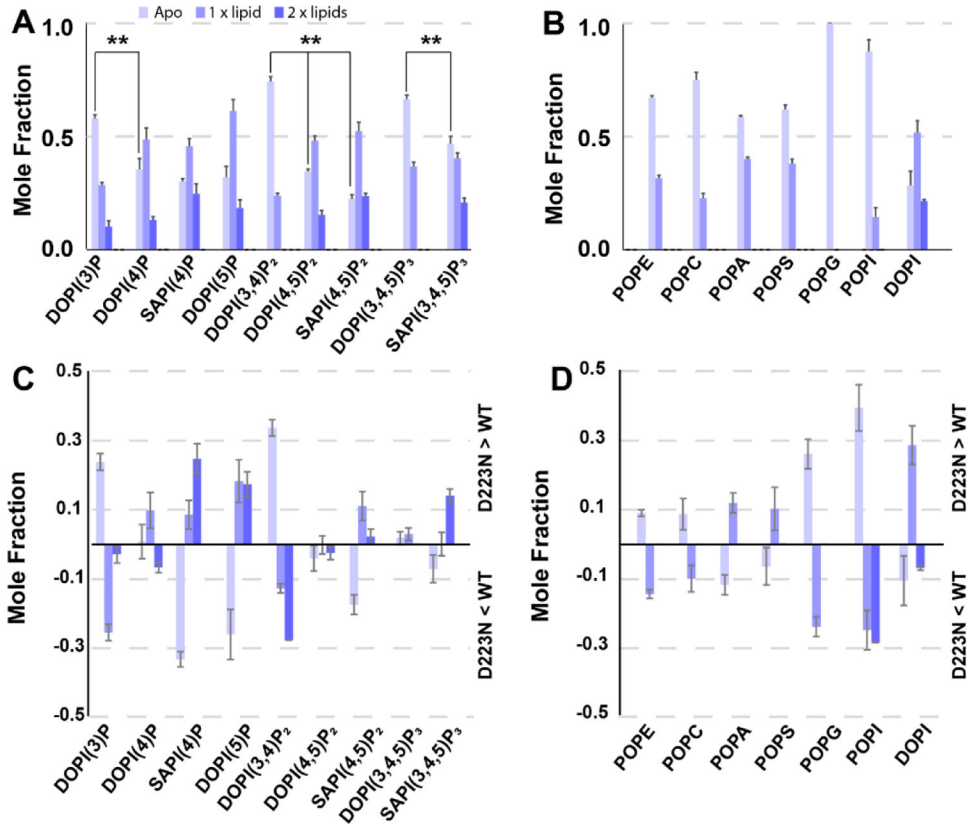

Figure 5. Native MS reveals Kir3.4^{D223N} enhanced binding to PIPs.

A-B) Plot of mole fraction for of apo and lipid-bound states of Kir3.4^{D223N} determined from the deconvoluted native mass spectra. Kir3.4^{D223N} was mixed with a 10-fold molar excess of (A) PIPs and (B) lipids. C-D) Plot of the difference in mole fraction of (C) PIPs and (D) lipids bound to Kir3.4^{D223N} from Kir3.4. Negative values indicate a higher mole fraction of the particular state for Kir3.4^{WT}. For comparison, student's *t* test (* *$p < 0.01$) was used with the apo mole fraction between indicated lipids. Reported are the average and s.e.m. (n=3).